

UC San Diego

UC San Diego Previously Published Works

Title

A Camptothetin Analog, Topotecan, Promotes HIV Latency via Interference with HIV Transcription and RNA Splicing

Permalink

<https://escholarship.org/uc/item/6px4x3fh>

Journal

Journal of Virology, 97(2)

ISSN

0022-538X

Authors

Mukim, Amey
Smith, Davey M
Deshmukh, Savitha
et al.

Publication Date

2023-02-28


DOI

10.1128/jvi.01630-22

Peer reviewed



A Camptothetin Analog, Topotecan, Promotes HIV Latency via Interference with HIV Transcription and RNA Splicing

Amey Mukim,^{a*} Davey M. Smith,^b Savitha Deshmukh,^{a§} Andrew A. Qazi,^a  Nadejda Beliakova-Bethell^{a,b,c}

^aVeterans Medical Research Foundation, San Diego, California, USA

^bDepartment of Medicine, University of California, San Diego, California, USA

^cVA San Diego Healthcare System, San Diego, California, USA

Amey Mukim and Davey M. Smith contributed equally to this work. Author order was determined both alphabetically and in order of increasing seniority.

ABSTRACT Low level HIV transcription during modern antiretroviral therapy (ART) in persons with HIV is linked to residual inflammation and associated diseases, like cardiovascular disease and cancer. The “block and lock” approach to hold HIV in a state of deep latency may help decrease residual inflammation in a person with HIV on ART and thus improve health. A camptothecin analog topotecan (TPT) was previously implicated as an inhibitor of active HIV replication. Using an *in vitro* primary T cell model of HIV latency, we demonstrated that (i) TPT reduces HIV transcriptional activity in latently infected cells; (ii) downregulation of HIV RNA by TPT cannot be reversed by latency reversing agents; (iii) several primary and secondary mechanism of action of TPT may be involved in control of HIV replication; (iv) regulation of HIV RNA by TPT is dependent on splicing complexity; (v) increase in proportion of unspliced HIV transcripts was facilitated by intron retention and upregulation of splicing factors, specifically *SRSF6*, by TPT. Although high TPT dosing (10 μ M) was needed to achieve the observed effects, viability of primary CD4⁺ T cells was not greatly affected. Because toxicity can be observed with TPT in persons with cancer, TPT is unlikely to be used as an anti-HIV agent in clinic, but our study provides proof that camptothetin has “block and lock” activity. Other camptothetin analogs, which are less toxic than TPT, should be designed and tested as HIV “block and lock” agents.

IMPORTANCE HIV survives in a state of very low activity, called latency, for long periods in persons with HIV on antiretroviral therapy. This low activity of HIV is linked to residual inflammation and associated diseases, such as heart disease and cancer. New strategies are being explored to further silence the HIV provirus and suppress residual inflammation. This study provides strong evidence that the camptothetin analog, Topotecan, can reduce residual activity of HIV in an experimental model of HIV latency. While Topotecan itself is likely not suitable for use in the clinic due to its toxicity, other camptothetin analogs should be designed and investigated as “block and lock” agents.

KEYWORDS HIV latency, Topotecan, block and lock, transcription, RNA splicing, intron retention, *SRSF6*

Modern antiretroviral therapy (ART) can successfully suppress the spread of HIV within a person, but the latent reservoir still persists in the form of integrated provirus (1). Cells containing latent provirus have basal transcriptional activity, causing residual HIV replication. This HIV replication during ART has been linked to systemic immune activation and inflammation (2–4). Increased inflammation promotes both the clonal expansion of infected T cells, thus maintaining the HIV reservoir (4), and several non-AIDS comorbidities, such as cardiovascular disease and cancer (5).

Multiple approaches to curing HIV have been proposed and attempted. One approach, commonly known as “shock and kill,” is based on proviral reactivation in the presence of

Editor Viviana Simon, Icahn School of Medicine at Mount Sinai

Copyright © 2023 American Society for Microbiology. All Rights Reserved.

Address correspondence to Nadejda Beliakova-Bethell, nbeliakovabethell@health.ucsd.edu.

*Present address: Amey Mukim, Beckman Coulter Life Sciences, Inc., Mississauga, Ontario, Canada.

§Present address: Savitha Deshmukh, StemCell Technologies, Inc., Vancouver, Canada.

The authors declare a conflict of interest. D.M.S. served as a consultant for Evidera, Matrix Biomed, Model Medicines, VxBio, Arena Pharmaceuticals, Pharma Holdings and Bayer Pharmaceuticals; served on the Scientific Advisory Board of Linear Therapies, Signant Health, and FluxErgy Inc. All other authors declare no conflict of interest.

Received 18 October 2022

Accepted 11 January 2023

Published 31 January 2023

ART, followed by elimination of infected cells by viral cytotoxicity or the immune system (6). This approach often uses latency reversing agents (LRAs) to disrupt the latent state of the provirus to initiate viral production, followed by immune clearance of infected cells. Unfortunately, this strategy has had limited success (7).

Another approach is “block and lock,” where HIV activation is blocked and the provirus is locked in a nonreplicative state (8). Although the “block and lock” approach would not eliminate the provirus, it has some advantages. First, it does not rely on the person’s immune system for HIV clearance after a “shock” treatment with an LRA. Second, the “block and lock” approach would not generate inflammatory responses like a “shock” treatment that could be detrimental in organs such as the brain (9). Third, “block and lock” is likely less invasive than gene therapy, chimeric antigen receptor T-cell therapy, and allogeneic stem cell transplantation cure strategies. Additionally, because HIV transcription is not completely suppressed with current ART regimens, a “block and lock” strategy that is adjunctive to ART may be useful by reducing residual inflammation and associated diseases, which is a major health issue for persons with HIV on modern ART (5).

Topotecan (TPT) is a semisynthetic drug derived from camptothecin that blocks the S-phase of cell cycle by inhibiting Topoisomerase I (10). It has been widely studied and is used clinically as a small molecule inhibitor for ovarian and small cell lung cancers (10). In the field of HIV research, early studies demonstrated that TPT slows the spread of infection by inhibiting HIV replication (11). This was independent of its ability to inhibit Topoisomerase I (12). More recently, the antiviral mechanism of action of a camptothecin analog (parent compound of TPT) was demonstrated to be through inhibition of HIV accessory protein, Vif (13). TPT was abandoned as an antiviral because of the much clearer utility of direct antiviral agents in the early 1990s. However, TPT may now be useful in the era of modern ART, as a “block and lock” strategy for HIV cure efforts and for blocking low-level HIV transcription that causes local inflammation and damage.

In this study, we investigated the antiviral effects of TPT using an *in vitro* primary T cell model of HIV latency (14–17). We demonstrated that TPT greatly decreases basal transcription in cells latently infected with HIV, even after treatment with several potent LRAs. Analysis of transcriptome remodeling by TPT using RNA-Seq indicated both direct effects of TPT on transcription, as well as indirect effects on HIV replication via modulation of cell signaling pathways. Moreover, we found that reduction of HIV RNA expression mediated by TPT was dependent on splicing complexity. We further determined that TPT may have several effects on splicing, including enhancement of intron retention and upregulation of splicing factors that favor generation of unspliced HIV RNAs. Our findings support the need for further studies of the camptothecin class of compounds for the “block and lock” approach of HIV latency.

RESULTS

Topotecan inhibits transcription in an *in vitro* primary CD4⁺ T cell model of HIV latency. Previous studies by Zhang et al. found antiviral effects of TPT using primary cells with acute HIV infection (12). To investigate the antiviral effects of TPT on latent HIV infection, we used an *in vitro* primary T cell model of latency (14–17). In this model, latent infection is established in primary CD4⁺ T cells in coculture with autologous activated, productively infected cells via cell-to-cell virus spread (17). Following latency establishment in this model, there is essentially no production of p24, but there are measurable low levels of HIV RNA (15, 17). Cells derived from this model were treated for 24 h with a broad dose range of TPT (1 nM, 10 nM, 100 nM, 1 μ M, and 10 μ M) in six replicate experiments. HIV GAG RNA and multiply spliced (MS) transcripts were significantly downregulated by both 1 nM and 10 μ M concentrations of TPT, compared to the solvent control, dimethyl sulfoxide (DMSO). The reduction in HIV RNA expression was most consistent across six replicates using the 10 μ M concentration of TPT (GAG, 25% \pm 10%, MS, 4% \pm 2%, $P < 0.001$), while reduction of HIV RNA expression with 1 nM TPT showed more variability (GAG, 53% \pm 21% $P < 0.001$; MS, 59 \pm 37, $P = 0.03$) (Fig. 1A). Overall, cell viability was only modestly decreased with increased concentrations

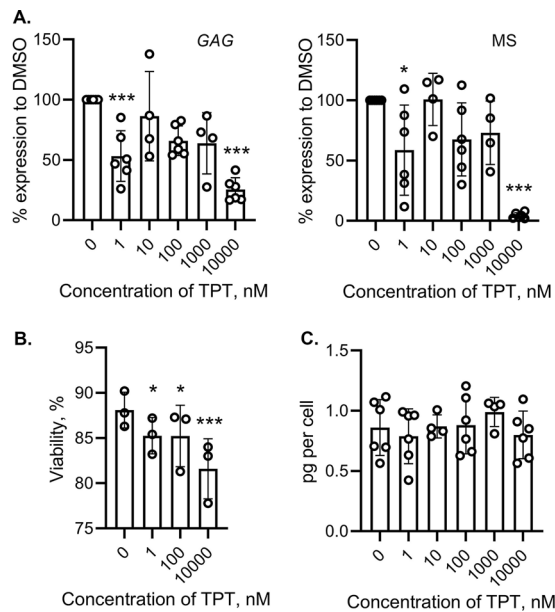


FIG 1 Downregulation of HIV RNA by TPT. (A) Unspliced (GAG) and multiply spliced (MS) transcripts were quantified by ddPCR, normalized to housekeeping gene *RPL27*, and presented as percent expression compared to DMSO control (0 nM TPT). (B) Viability was quantified using Aqua Live/Dead staining and cells from 3 donors. (C) RNA yields per cell (pg per cell) were determined by multiplying RNA concentration (quantified using Qubit) by extraction volume and divided by the number of collected cells. In A and C, the entire range of TPT concentrations was used for four out of six replicate experiments, 10 nM and 1,000 nM were omitted due to cell number constraints. In all graphs, mean and standard deviation are shown for three to six replicate experiments with CD4⁺ T cells obtained from different blood donors, individual data points are shown. Error bars represent standard deviation. Asterisks indicate significant difference compared to DMSO controls (0 nM TPT); *, $P < 0.05$; ***, $P < 0.001$.

of TPT (88% viability with DMSO, 85% at 1 nM and 100 nM TPT, and 82% at 10 μ M TPT) (Fig. 1B).

Topotecan perturbs transcriptional processes and signaling pathways. To test whether the observed decrease in HIV transcription represented specific TPT effect on HIV versus inhibition of transcription globally, total RNA yields were first compared between the treated and untreated conditions. Here, we found that overall RNA yields were not dependent on TPT dosing (Fig. 1C).

Because overall RNA yields were similar, we hypothesized that TPT had differential impact on the host transcriptome. To investigate this hypothesis, we conducted RNA-Seq using the *in vitro* model of HIV latency set up with cells obtained from three different blood donors. Cells were treated with solvent control DMSO versus 10 μ M TPT. Differential gene expression analysis identified 522 genes that were upregulated by TPT, while 1,227 genes were downregulated (Table S1). To determine which biological processes and pathways were affected by TPT, gene ontology (GO) terms and pathway enrichment analysis was conducted using the Database for Annotation, Visualization and Integrated Discovery (DAVID) v2022q3 (18) (Tables S2 and S3). Consistent with its known Topoisomerase I inhibition activity, treatment with TPT induced DNA damage responses, evident from pathways *DNA Damage/Telomere Stress Induced Senescence* and *G2/M DNA damage checkpoint* being enriched for differentially expressed genes (Table S2). We also found that TPT modulated transcriptional processes, including upregulation of histone genes and downregulation of multiple genes that encode proteins involved in regulation of transcription (Tables S2 and S3 and Fig. 2). Several signaling pathways, including T cell receptor signaling, positive regulation of JNK cascade, regulation of actin cytoskeleton, and positive regulation of GTPase activity were affected by TPT treatment (Table S2; Fig. 3).

Topotecan affects alternative splicing of HIV RNA. Because MS transcripts were downregulated to a greater extent compared to unspliced HIV RNA (GAG) (Fig. 1A), we

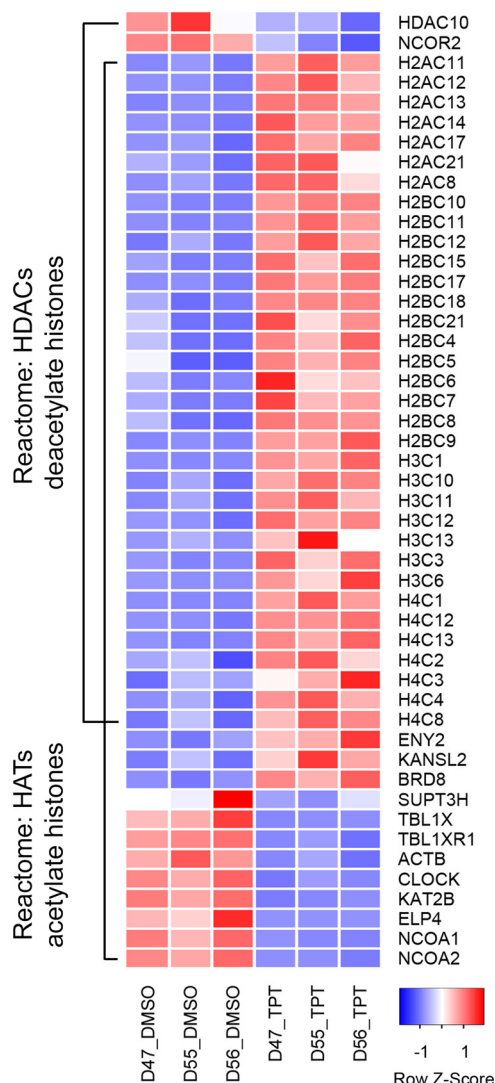


FIG 2 Interference of TPT with genes involved in regulation of transcription. RNA-Seq was conducted using cells from three different blood donors, and differentially expressed genes were identified between samples treated with 10 μ M TPT and DMSO solvent control. A number of pathways and biological processes involved in regulation of transcription were identified (Tables S2 and S3); upregulation of histone genes and downregulation of chromatin modifying enzymes in Reactome pathways are shown. Heatmap was constructed using function *heatmap.2* from the library *gplots* in R. For the heatmap construction, samples were arranged by group (DMSO followed by TPT); construction of dendrograms was omitted. Gene expression was scaled by row; scale bar represents scaled gene expression values.

hypothesized that TPT may be affecting alternative splicing. To test this hypothesis, we performed a dose range study where cells from our primary cell latency model were treated with 1 μ M and 10 μ M TPT and then assayed for unspliced (*GAG*), singly spliced (*ENV*) and MS HIV transcripts, representing an increase in splicing complexity. No effect was observed at the 1 μ M dosing, but at 10 μ M TPT dose splicing complexity (MS transcripts) was clearly inhibited. Specifically, expression of *GAG* RNA ranged between 17% and 42% ($P < 0.001$), *ENV* RNA between 6 and 36% ($P < 0.001$), and MS RNA between 2% and 8% ($P < 0.001$), compared to expression in samples treated with DMSO.

To begin to understand the mechanism by which TPT downregulated different HIV transcripts, we quantified the change in proportion of each transcript following 1 μ M and 10 μ M treatment with TPT. While no changes were seen at 1 μ M dose, treatment with 10 μ M TPT resulted in an average increase in unspliced transcripts (*GAG*) from 48.5% to 61.5% ($P < 0.001$), while singly spliced (*ENV*) and MS transcripts decreased on average from 44.9% to 37.0% ($P < 0.001$) and from 6.6% to 1.4% ($P < 0.001$) (Fig. 4).

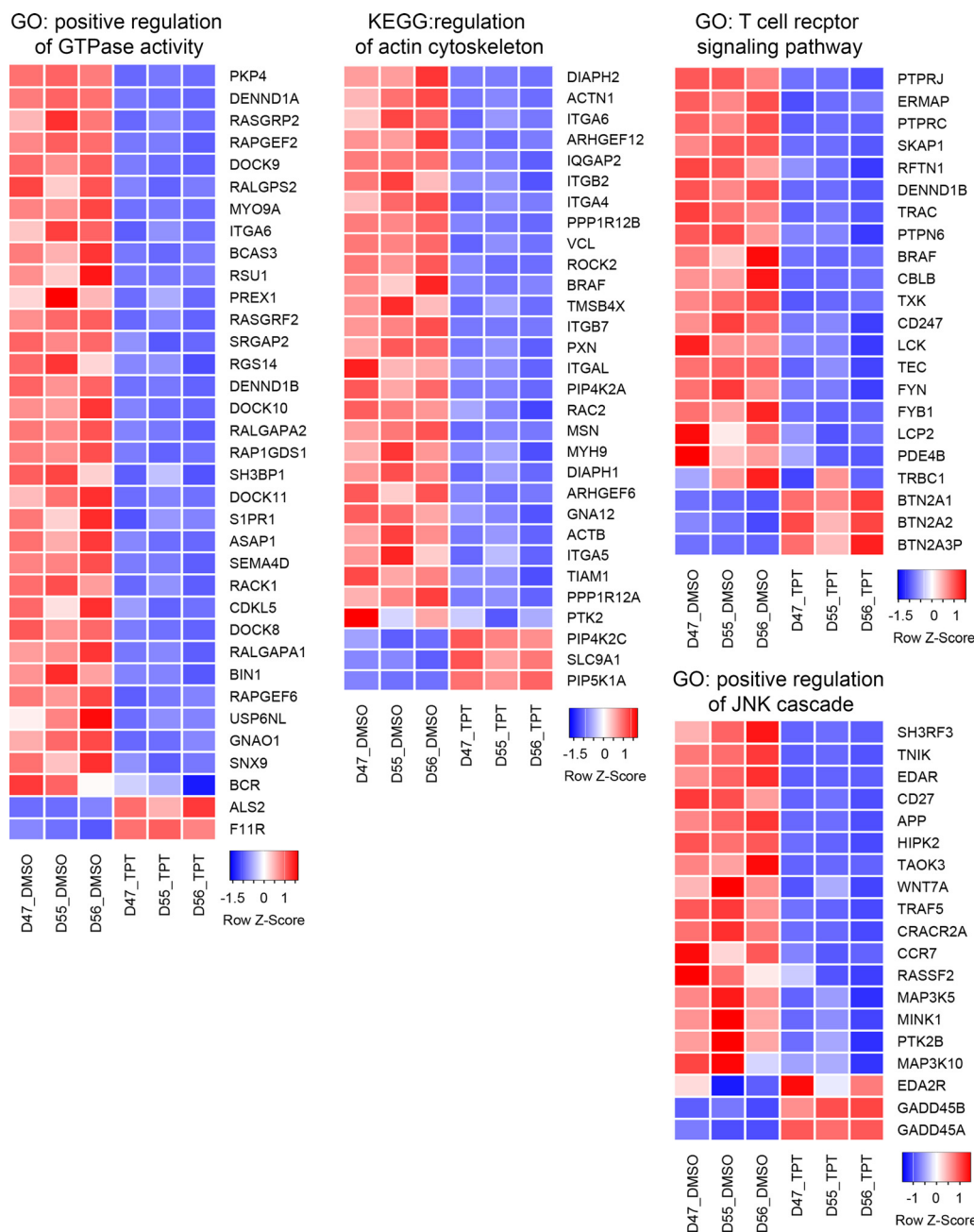


FIG 3 Interference of TPT with signaling pathways. RNA-Seq was conducted using cells from three different blood donors, and differentially expressed genes were identified between samples treated with 10 μ M TPT and DMSO solvent control. Biological process GO terms and a KEGG pathway are presented. Heatmaps were constructed using function *heatmap.2* from the library *gplots* in R. For the heatmap construction, samples were arranged by group (DMSO followed by TPT); construction of dendrograms was omitted. Gene expression was scaled by row; scale bars represent scaled gene expression values.

Because during eukaryotic RNA production splicing occurs simultaneously with native RNA transcription, the observed synchronous accumulation of *GAG* and reduction of spliced RNA species is consistent with dysregulation of alternative splicing pathways.

Mechanisms of dysregulation of alternative splicing pathways by Topotecan.

Based on the evidence that TPT is likely to dysregulate alternative splicing pathways, we hypothesized two possible mechanisms that may explain the observed preferential reduction of the MS transcripts: (i) TPT promotes intron retention or (ii) TPT affects expression of host genes that regulate HIV splicing.

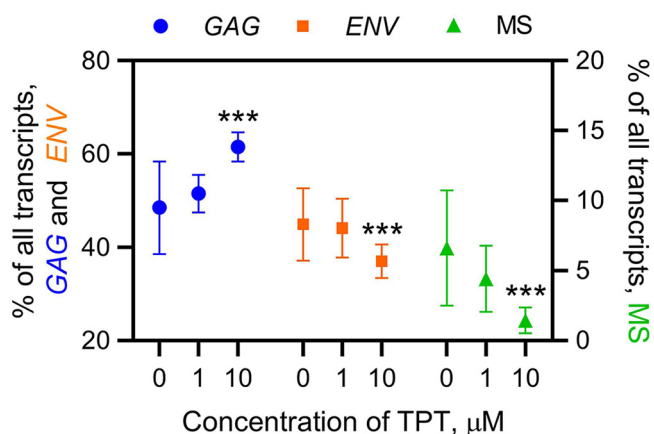


FIG 4 Accumulation of unspliced and reduction in proportion of spliced HIV transcripts following treatment with TPT. Transcripts of HIV (*GAG*, *ENV*, and *MS*) are presented as percentage of all HIV transcripts quantified by ddPCR and normalized to housekeeping control *RLP27*. Following treatment with 10 μM TPT, proportion of unspliced transcripts increases, while proportion of spliced forms decreases. This effect is more pronounced for *MS* compared to singly spliced transcript *ENV*. Error bars represent standard deviation. Asterisks indicate significant difference compared to DMSO controls (0 nM TPT); ***, $P < 0.001$.

Intron retention is a rare event among vertebrate genes, with only nine cases confirmed experimentally (18). In humans, intron retention has been reported for four cases: (i) serine and arginine rich splicing factor 7 (*SRSF7*), previously known as 9G8 (19); (ii) TGF β -induced factor homeobox 2 (*TGIF2*) (20); (iii) thrombopoietin (*THPO*, previously known as *TPO*) (21); and (iv) kallikrein gene family (22). To select a suitable target in our experiments, expression of human genes with reported intron retention events was evaluated in human primary CD4⁺ T cells using our RNA-Seq data. Expression of kallikerins and *THPO* was not detected, while *TGIF2* was detected and a low level. The only gene that was expressed at a high level, sufficient for detection by droplet digital PCR (ddPCR), was *SRSF7*. In this gene, the intron retention event is in the intron between exons 3 and 4, and there is a possible alternative splice site from exon 3 (19). We, therefore, quantified the main spliced transcript, the alternatively spliced transcript, and the transcript with intron retention at this position in uninfected CD4⁺ T cells treated with 1 μM and 10 μM TPT, compared to DMSO controls. Both spliced transcripts of *SRSF7* were downregulated in TPT-treated samples (expression level relative to DMSO control was 56% \pm 27% [$P < 0.001$] and 44% \pm 17% [$P = 0.64$] with 1 μM ; 20% \pm 5% [$P < 0.001$] and 15% \pm 17% [$P < 0.001$] with 10 μM TPT) (Fig. 5A). The transcript of *SRSF7* with intron retention was modestly upregulated (expression level relative to DMSO control was 130% \pm 33% [$P = 0.17$] with 1 μM and 130% \pm 45% [$P = 0.19$] with 10 μM TPT) (Fig. 5A). This observation is not consistent with the idea that intron retention caused by TPT is specific for HIV but rather affects host gene transcripts as well.

Another possible mechanism of action of TPT is the effect on HIV splicing efficiency. There are 12 canonical splicing factors, *SRSF1* through 12, many of which regulate HIV splicing (reviewed in reference 23). We were interested in testing how TPT affects *SRSF4* and *SRSF6* because these factors act to increase the abundance of unspliced HIV RNA in the cytoplasm (24, 25). Using ddPCR, we found that expression of both of these splicing factors at the RNA level was elevated in the TPT-treated samples (Fig. 5B). Expression level relative to DMSO control for *SRSF4* was 149% \pm 48% ($P = 0.07$) with 1 μM and 177% \pm 100% ($P = 0.012$) with 10 μM TPT. Expression level relative to DMSO control for *SFRS6* was 199% \pm 120% ($P = 0.025$) with 1 μM and 253% \pm 80% ($P < 0.001$) with 10 μM TPT (Fig. 5B). In a separate experiment, using cells from three different donors, expression of *SRSF4* and *SRSF6* was assessed at the protein level using immunoblot. After treatment with 1 μM TPT, no differences in expression were observed, while with 10 μM TPT treatment, expression of protein encoded by *SRSF6*, but not *SRSF4*, was elevated (176% \pm 74%, $P = 0.008$) (Fig. 5B). To further link changes

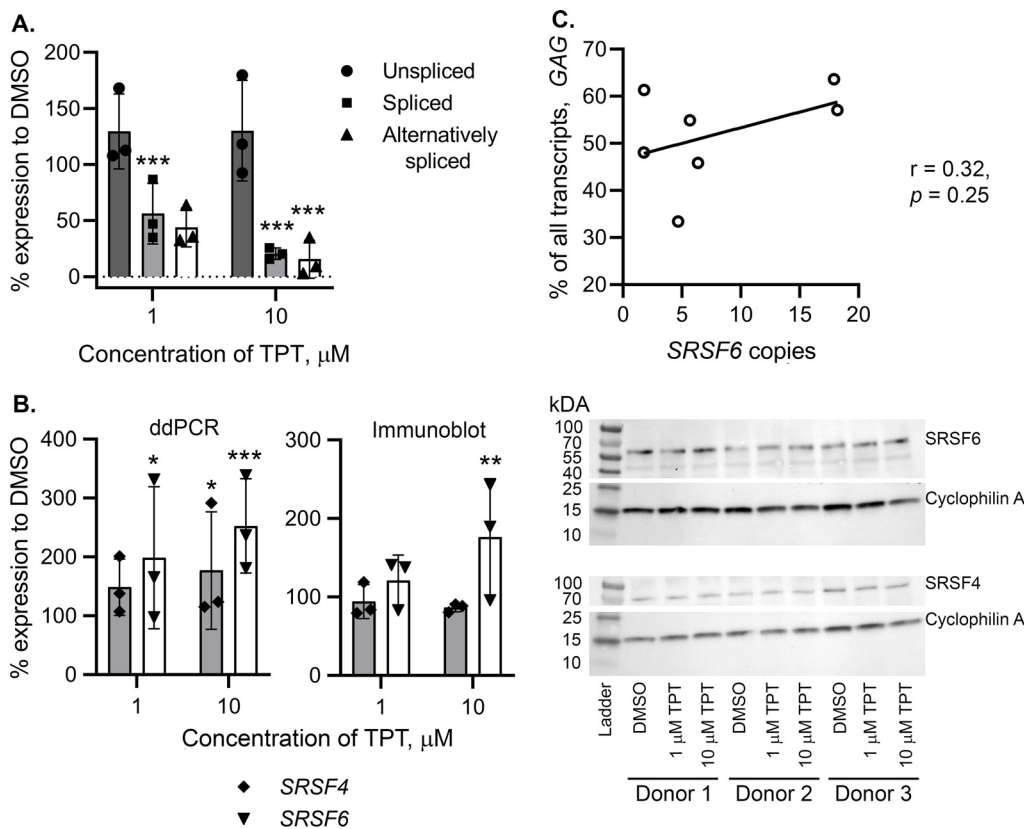


FIG 5 Mechanisms of splicing regulation by TPT. (A) TPT promotes intron retention. Different *SRSF7* isoforms were quantified by ddPCR, demonstrating modest upregulation of transcripts with intron retention between exons 3 and 4, and downregulation of spliced transcripts. (B) TPT upregulates splicing factor *SRSF6* both at the RNA and protein levels, and *SRSF4* at the RNA level only. Transcripts were quantified by ddPCR (left graph), and protein was quantified by immunoblot (right graph). In all graphs, mean and standard deviation of percent expression relative to DMSO solvent control are shown in triplicate experiments with $CD4^+$ T cells obtained from different blood donors; individual data points are shown. Error bars represent standard deviation. Asterisks indicate significant difference compared to DMSO controls (0 nM TPT); *, $P < 0.05$; **, $P < 0.01$; ***, $P < 0.001$. Raw immunoblot data are presented on the right. (C) Spearman correlation analysis between expression of *SRSF6* (copies per 10^3 molecules of housekeeping control *RPL27*) and proportion of GAG transcripts among all HIV transcripts. All available samples treated with DMSO ($N = 3$), 1 μ M TPT ($N = 1$) and 10 μ M TPT ($N = 3$) were used for this analysis.

in expression of *SRSF6* and HIV splicing, correlation analysis between *SRSF6* expression and proportion of GAG transcripts was conducted. We observed a modest ($r = 0.32$) insignificant ($P = 0.25$) positive correlation between these variables (Fig. 5C), consistent with the idea that some variance in the proportion of GAG transcripts may be explained by differences in *SRSF6* expression, but more samples may be needed to evaluate this relationship. We next evaluated expression of all 12 SRSF genes in our RNA-Seq data. *SRSF12* was not detected, and among the 11 detected genes many were modestly up-regulated (less than 1.5-fold, false discovery rate [FDR]-corrected $P < 0.05$) (Table 1). Altogether, these results are consistent with the idea that TPT interferes with HIV splicing via modulating host splicing factors.

“Block and lock” effects of Topotecan are not reversed by latency reversing agents. To test the effect of TPT on HIV transcription, we used LRAs with a variety of mechanisms of action: (i) protein kinase C (PKC) agonists bryostatin, phorbol myristate acetate (PMA) and prostratin; (ii) histone deacetylase inhibitors (HDACis) Romidepsin and suberoylanilide hydroxamic acid (SAHA); (iii) T cell receptor (TCR) signaling activator, phytohemagglutinin M (PHA-M); and (iv) TNF receptor-associated factor (TRAF) recruiter, tumor necrosis alpha (TNF- α). Cells derived from the latency model were treated with LRAs in the presence and absence of TPT (10 μ M). As might be expected, LRA treatment alone caused an increase in HIV RNA levels in the latency model, but

TABLE 1 Expression of the SRSF genes from the RNA-Seq experiment

ENSEMBL ID	Gene symbol ^a	Fold change ^b	P value	FDR ^c
ENSG00000111786	SRSF9	1.50	4.95E-08	1.42E-07
ENSG00000136450	SRSF1	1.42	4.96E-09	1.56E-08
ENSG00000188529	SRSF10	1.42	6.87E-09	2.13E-08
ENSG00000100650	SRSF5	1.41	1.43E-05	3.15E-05
ENSG00000116754	SRSF11	1.34	3.08E-06	7.33E-06
ENSG00000124193	SRSF6	1.33	3.60E-06	8.51E-06
ENSG00000161547	SRSF2	1.29	1.26E-04	2.48E-04
ENSG00000116350	SRSF4	1.17	1.22E-02	1.85E-02
ENSG00000115875	SRSF7	1.14	3.71E-02	5.21E-02
ENSG00000263465	SRSF8	-1.09	1.49E-01	1.86E-01
ENSG00000112081	SRSF3	-1.12	6.21E-02	8.37E-02

^aOfficial gene symbol.

^bFold change in expression in samples treated with 10 μ M TPT relative to the solvent control DMSO.

^cFalse discovery rate corrected P value.

this effect was abrogated across the board when the cells were also treated with TPT (Fig. 6A and B).

For the proof-of-principle that TPT suppresses HIV transcription for an extended period of time, a cell line model of HIV latency, the JLat clone 6.3, was treated with TPT for 24 h, and then cultured in the absence of TPT for 3 days. Cells that were treated with the solvent DMSO were used as a control. During TPT treatment, and every day following removal of TPT from culture, cells were treated with TNF- α for 24 h. Induction of HIV expression was monitored using expression of the green fluorescent protein (GFP) reporter introduced into the HIV genome in this cell line (see Fig. 6C for experimental design). For the entire duration of the time course, production of GFP was reduced to similar levels in cells pretreated with TPT, compared to DMSO controls (Fig. 6D). These results are consistent with the idea that inhibition of HIV gene expression remains for at least 3 days following TPT removal.

DISCUSSION

Permanent or long-term silencing of the HIV provirus can be achieved by targeting factors that are known to control and stabilize HIV latency. For example, absence of Tat and other long terminal repeat (LTR) regulators of HIV (e.g., TAR hairpin) can inhibit HIV transcriptional initiation and elongation, and push latent provirus into a state of deeper latency (26, 27). A proof-of-concept study demonstrated that Tat inhibitor didehydro-Cortistatin A suppressed HIV transcription via epigenetic silencing at the LTR (28, 29). Most recently, a new small molecule compound, Q308, was shown to suppress HIV in a Tat-dependent manner via enhancing Tat proteasomal degradation (30). Though targeting Tat is an excellent choice for a “block and lock” approach, the nature of Tat/TAR feedback circuit presents a limitation in that targeting Tat may require prolonged treatment or involve a combination of targets (31). To increase the probability of success of “block and lock” strategy for HIV cure, investigating other viral and cellular targets is crucial.

The present study evaluated the value of TPT as a “block and lock” agent. We demonstrated that: (i) TPT reduces HIV transcription in latently infected cells (Fig. 1); (ii) downregulation of HIV gene expression caused by TPT cannot be reversed by LRAs in a primary T cell and a cell line models of HIV latency (Fig. 6); (iii) several primary and secondary mechanism of action of TPT may be involved in control of HIV replication (Fig. 2 and 3; Tables S2 and S3); (iv) regulation of HIV transcription by TPT is dependent on splicing complexity (Fig. 4); and (v) increase in proportion of unspliced HIV transcripts (Fig. 4) was facilitated by intron retention and upregulation of splicing factors, specifically *SRSF6*, by TPT (Fig. 5; Table 1).

Antiviral action of another camptothecin derivative O2-16, was previously suggested to be via inhibition of Vif and protection of APOBEC3G from Vif-mediated degradation (13). While we did not evaluate TPT effects on Vif and protection of APOBEC3G, our data indicate that TPT treatment effectively inhibits HIV RNA transcription during

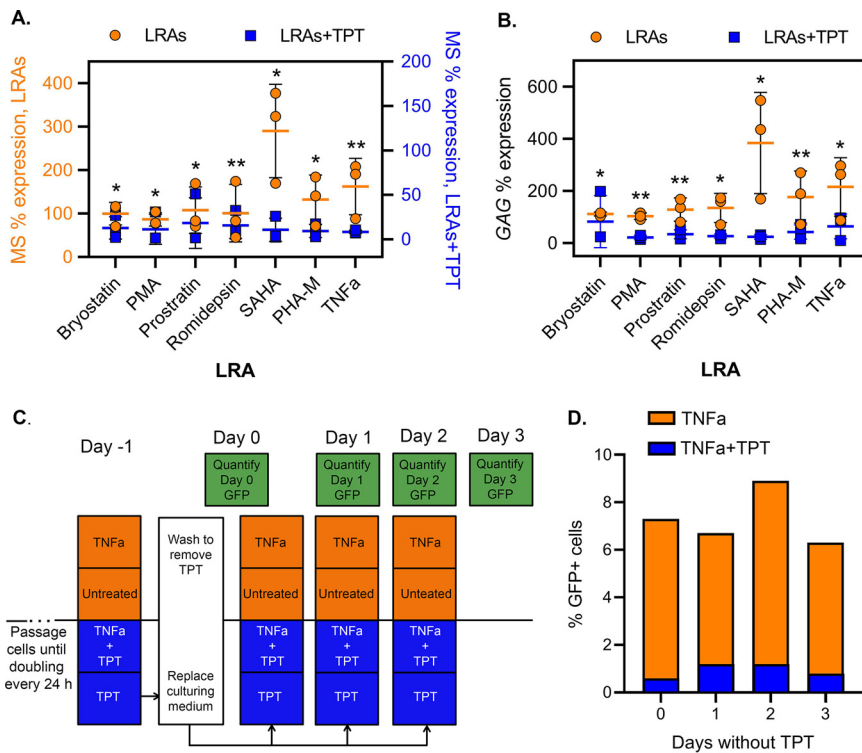


FIG 6 TPT inhibits potency of LRAs. (A and B) Experiment was performed using primary CD4⁺ T cell model of HIV latency set up using cells from three different blood donors. Reactivation capacity of several LRAs was tested in the absence (orange circles), or presence (blue squares) of 10 μM TPT; mean and standard deviation are shown. Asterisks indicate significant difference between LRA-treated and LRA+TPT-treated groups; *, $P \leq 0.05$; **, $P < 0.01$. (A) Percent expression of MS transcript relative to DMSO; (B) Percent expression of GAG transcript relative to DMSO. (C) Experimental design to evaluate the effect of TPT on HIV gene expression following removal of TPT from culture. JLat cell line model of HIV latency (clone 6.3) was used for these experiments. Cells were treated with TPT for 24 h (blue boxes); TPT was washed out, and cells were cultured in the absence of TPT for 3 additional days. Cells treated with DMSO solvent were used as control (orange boxes). Every day aliquots of cells from both TPT- and DMSO-treated conditions were used to activate HIV gene expression using TNF-α, and for untreated controls. The next day, cells were evaluated for expression of the GFP reporter protein using flow cytometry. (D) TPT inhibited HIV reactivation with TNF-α over the 3-day time course. At each time point, percentage of cells positive for GFP following treatment with TNF-α was normalized to percentage of cells positive for GFP expression in TNF-α-treated samples minus percentage of cells positive for GFP expression in untreated samples.

latency (Fig. 1A). In addition to reducing baseline transcription, TPT was able to block reactivation of HIV transcripts when LRAs with different mechanisms of action were used. Because neither spliced (MS) or unspliced (GAG) transcripts could be reactivated with either of the LRAs tested in the presence of TPT (Fig. 6), TPT is likely to act at the stage of transcription initiation or elongation. Our RNA-Seq analysis indicated that TPT treatment influenced multiple genes involved with transcriptional regulation, including upregulation of genes that encode histone proteins and downregulation of chromatin modifying enzymes and other transcription factors (Fig. 2). Furthermore, TPT treatment interfered with a number of pathways important for HIV replication, including T cell receptor, JNK, and GTPase signaling and regulation of actin cytoskeleton (32–35). Together, these TPT-mediated effects represent potential secondary mechanisms of action by which HIV provirus is maintained in an inactive state. Some of these secondary effects seem to also interfere with the ability of LRAs to reactivate HIV transcription.

In addition, we observed that TPT treatment caused synchronous accumulation of unspliced HIV transcripts (Fig. 4). Of the two splicing factors tested, *SRSF4* and *SRSF6*, which promote accumulation of unspliced HIV RNA (24, 25), upregulation of *SRSF6* by TPT treatment was consistent at both RNA and protein level. Moreover, expression of

SRSF6 modestly correlated with accumulation of unspliced HIV RNA. This observation is consistent with a prior report that demonstrated *SRSF6* promoted production of incompletely spliced huntingtin transcripts (36). It is thus plausible that TPT promotes intron retention in part via upregulation of *SRSF6*. The effect of TPT treatment on intron retention also seemed to apply to host genes as well, for example *SRSF7* (Fig. 5A). Altogether, our results demonstrate antiviral mechanisms of TPT other than Vif inhibition.

Overall, our results are consistent with TPT regulating HIV expression at multiple levels, but limitations remain. One limitation is that posttranslational effects have not been evaluated, and identification of posttranslational mechanisms of action might be important for development of additional treatment targets. Another limitation of our study is the short-term culture of cells following TPT treatment, as longer term treatment with a camptothetin class of drugs would likely be needed. Along these lines, it is unclear if the repression of HIV transcription would occur in a person with HIV and whether this repression would decrease inflammation and improve health. Long-term studies will also be needed to evaluate the ability of TPT to suppress proviral reactivation with LRAs. A general limitation of using TPT is its high concentration at which the effects on HIV transcription and splicing were considerable and consistent. Even though we did not see much of an effect on viability of CD4⁺ T cells (Fig. 1B), a clinical trial using TPT to treat progressive multifocal leukoencephalopathy in persons with HIV demonstrated toxicity, in particular anemia, neutropenia, and thrombocytopenia (37).

Thus, TPT is not likely to be a useful “block and lock” therapy, but this study was a proof-of-concept that camptothetin analogs can serve this purpose, and similar but less toxic drugs should be identified and tested. Although advances in ART have been successful in reducing mortality and controlling viral rebound, low level of HIV transcriptional activity causing residual inflammation continues to be a problem (2, 5). Having an adjunctive therapy that could stop such HIV transcription and thus inflammation is important in the next generation of HIV treatment. Our findings suggest that TPT-like drugs may serve this purpose.

MATERIALS AND METHODS

Study participants. Whole blood from HIV seronegative donors was used to isolate primary CD4⁺ T cells for this study. The protocol was approved by the Institutional Review Board of the University of California San Diego. All volunteers provided written informed consent to participate.

Isolation of CD4⁺ T cells. For all experiments that involved *in vitro* infection with HIV, buffy coat was obtained from whole blood of healthy donors using Lymphoprep (StemCell Technologies, Inc., Vancouver, Canada). CD4⁺ T cells were isolated using negative selection kit (StemCell Technologies, Inc., Vancouver, Canada). Quality control check was performed to assess sample purity (>95% CD4⁺) and expression of activation marker HLA-DR (<10%) using the Accuri C6 flow cytometer (BD Biosciences, Inc., San Jose, CA, USA). For experiments with uninfected CD4⁺ T cells, cryopreserved cells were used.

The *in vitro* model of HIV latency. Viral stocks were prepared by transfecting CEM T lymphoblastoid cell line as described (38) and quantified for infectivity by the P4R5 MAGI blue cell assay (39). Latently infected primary CD4⁺ T cells were generated using an *in vitro* model of HIV latency, as described previously (14–17). Briefly, following isolation, 80% of CD4⁺ T cells were set aside for 5 days without infection or stimulation (“resting”). The other 20% were labeled with a cell tracking dye (e-flour 670, Thermo Fisher Scientific, Inc., Waltham, MA, USA), held overnight, and infected in aliquots of 4 to 6 × 10⁶ cells for 4 h to 6 h using wild-type HIV_{NL4-3} at the multiplicity of infection 0.005 infectious units. Postinfection, cells were extensively washed with phosphate-buffered saline containing 2% human serum and stimulated using plate bound αCD3/CD28 antibodies for 4 days. These autologous productively infected cells were mixed with uninfected resting cells at a ratio of 1:4 and cultured in IL-2/IL-15 rich media to facilitate cell-to-cell virus transmission and establishment of latent infection in resting cells. After 3 days of coculture, resting e-flour negative cells were sorted by means of flow cytometry using either a MoFlo XDP cell sorter (Beckman Coulter, Brea, CA, USA), or a FACS Aria II instrument (BD Biosciences, Inc., San Jose, CA, USA). Cells were cultured for 3 additional days to complete viral integration, at which point they were ready for cell assays.

The cell line model of HIV latency. The cell line JLat clone 6.3, developed in the laboratory of Dr. Verdin (40) was obtained through the NIH AIDS Reagents Program. This cell line has an integrated HIV provirus with the GFP reporter cloned in place of *nef*, which allows tracking HIV expression using flow cytometry. Cells were passaged in RPMI medium containing 10% fetal bovine serum until they doubled every 24 h. Culture media was changed every 48h to 72 h and prior to drug treatments, with starting cell concentration 300,000 cells per mL. Cell count and viability were accessed using hemocytometer and 0.04% trypan blue exclusion dye (Thermo Fisher Scientific, Inc., Waltham, MA, USA).

Drug treatment. TPT, PHA-M, PMA, Prostratin, Bryostatin (Sigma-Aldrich, LLC, St. Louis, MO, USA), SAHA and Romidepsin (Selleck Chemicals, LLC, Houston, TX, USA) were solubilized in DMSO. TNF- α (Peprotech, Inc., Rocky Hill, NJ, USA) was solubilized in water. For cytotoxicity and dose response studies, cells derived from the latency model were treated with TPT (1 nM to 10 μ M) for 24 h. Reactivation of latently infected cells using LRAs, in the presence and absence of TPT, was performed for 24 h (Bryostatin [33 nM], PMA [2 nM], Prostratin [100 nM], Romidepsin [15 nM], SAHA [300 nM], PHA-M [33 μ g/mL]) and 48 h (TNF- α [0.2 ng/mL]). Each treatment was initially set up using 500,000 cells. At harvest, cells were counted using the Accuri C6 flow cytometer (BD Biosciences, Inc., San Jose, CA, USA) and bead standards (Thermo Fisher Scientific, Inc., Waltham, MA, USA). RNA extraction was performed using Qiagen RNeasy RNA extraction kit (Qiagen, Inc., Valencia, CA, USA). Cell viability following treatment with TPT was assessed using the live/dead fixable dead-cell stain kit (Thermo Fisher Scientific, Inc., Waltham, MA, USA). The JLat 6.3 cell line was treated with 10 μ M TPT or its solvent DMSO for 24 h. Aliquots of cells treated with TPT were used to treat (or not) cells with TNF- α (10 ng/mL), in parallel with TPT treatment, to collect baseline data on the levels of inhibition of HIV expression by TPT. Each treatment had initially 300,000 cells. The following day, baseline samples were accessed for GFP expression using the Accuri C6 flow cytometer (BD Biosciences, Inc., San Jose, CA, USA). The cells treated with TPT were washed and resuspended in fresh medium. Every day for additional 3 days, aliquots were taken to treat (or not) these cells with TNF- α for 24 h, and GFP expression data were collected the following day.

Isolation and quantification of RNA. RNA was isolated from primary CD4⁺ T cells using RNeasy micro kit (Qiagen, Inc., Valencia, CA, USA). RNA concentrations were assessed using Qubit 2.0 fluorometer (Thermo Fisher Scientific, Inc., Waltham, MA, USA). RNA yields were calculated as RNA concentration multiplied by extraction volume divided by the number of cells from which RNA was extracted.

RNA-Seq. RNA-Seq experiment was conducted using the *in vitro* model of latency treated with 10 μ M TPT and DMSO solvent control, generated from three different blood donors. Cells collected for RNA-Seq experiments were lysed using RLT buffer from the RNeasy micro kit, and ERCC spike-in RNA (Thermo Fisher Scientific, Inc., Waltham, MA, USA) was added to cell lysates prior to RNA isolation. Even though RNA yields were similar, we reasoned that using spike-in RNA will serve as additional validation that TPT does not induce global gene expression inhibition. Following isolation, RNA integrity was assessed using an Agilent TapeStation and deemed of good quality for conducting an RNA-Seq experiment; RNA integrity numbers were an average 9.25 ± 0.08 . RNA-Seq was performed at the Institute of Genomics Medicine (IGM) Genomics Center at the University of California San Diego. Libraries were prepared using 100 ng of RNA as a starting material and the TruSeq Stranded Total RNA Library Prep kit (Illumina, Inc., San Diego, CA). Libraries were sequenced on the NovaSeq 6000 instrument (Illumina, Inc., San Diego, CA) to generate 100-bp paired end library reads. FASTQ files are available through the Gene Expression Omnibus (GEO) database, accession number [GSE215461](https://www.ncbi.nlm.nih.gov/geo/query/acc.cgi?acc=GSE215461).

Data preprocessing included filtering of low-quality reads and removal of 3' adapter sequences using the Trim Galore tool, which utilizes the Catadapt program (41). Reads were mapped to the human genome hg38 (GRCh38, p13) using HISAT2 (42). Mapped reads were counted against the human GENCODE annotation (v37) (43) using HT-Seq (44). ERCC scaling factors were calculated as described (45, 46). The range of scaling factors was 0.72 to 1.16, consistent with the idea that TPT did not induce global inhibition of gene expression. Therefore, all further analyses were conducted without adjusting gene read counts based on ERCC reads. The *EdgeR* library (47) in the R computing environment was used for differential gene expression analysis. EdgeR uses empirical Bayes estimation and exact tests based on the negative binomial distribution of the RNA-Seq read data, followed by the FDR correction using the Benjamini-Hochberg method (48). Genes were considered significantly modulated by TPT when FDR-corrected *P*-values were < 0.05 . To reduce the number of false positives, genes were also filtered by the fold change in expression (absolute fold change > 2).

Pathways and GO terms overrepresented for differentially expressed genes were identified using the Database for Annotation, Visualization and Integrated Discovery (DAVID) v2022q3 (49). All genes with FDR-corrected *P*-values < 0.05 and absolute fold change > 2 were used as input. DAVID uses a one-sided Fisher's exact test for gene set enrichment analysis. Pathways and GO terms with FDR-corrected *P*-values < 0.05 were considered significantly enriched for differentially expressed genes.

Droplet digital PCR. RNA (20 to 60 ng) was reverse transcribed using cDNA synthesis kit (Quanta Bio, Inc., Beverly, MA, USA). ddPCR was performed as described previously (14), using host gene ribosomal protein L27 (*RPL27*, assay HS03044961_g1, Applied Biosystems, now Thermo Fisher Scientific, Inc., Waltham, MA, USA) as normalization control in all experiments with resting cells. When cells were activated by LRAs, HIV RNA expression was normalized to cell input into reactions. To quantify HIV RNA, *GAG*, *ENV*, and *MS* assays (14) were used. Selection of host genes for intron retention study was based on expression level likely detectable in a single ddPCR reaction (number of reads per base in the RNA-Seq experiment greater than 0.5). Reads per base were calculated by dividing the number of reads mapped to each of the genes with reported intron retention events over the average transcript length as determined by the *GenomicFeatures* library (50) in Bioconductor R. The assays to quantify different transcripts of the selected gene *SRSF7* were obtained from Integrated DNA Technologies, Inc. (Coralville, IA, USA): assay for retained intron between exons 3 and 4- forward, 5'-GCCTTGCAAATCCGACAATTA-3'; reverse, 5'-GGTGAAGCTAGGTGTAGATGAC-3'; probe, 5'-TCCTCTAGACCTTGAGGTGATCAGC-3'; assay spanning exons 3 and 4- forward, 5'-ATGCTATGAGTGTGGCGAAA-3'; reverse, 5'-CTTCTCTGGATCGAGAATGTG-3'; probe, 5'-CGAAGAAGAAGCAGGTACGGTCT-3'; assay spanning exon 3 and alternate exon 4- forward, 5'-TGCTTATGATTGTCATCGTTACAG-3'; reverse, 5'-CCCAATTGTAAGCCAAATTTACTG-3'; probe, 5'-CAAATTCTCTGCCCTGCTTCTCTTCG-3'. The assays for *SRSF4* (Hs00900675_m1) and *SRSF6* (Hs00740177_g1) were from Applied Biosystems (now Thermo Fisher Scientific, Inc., Waltham, MA, USA).

Immunoblotting. Uninfected primary cells obtained from three different blood donors were treated with DMSO or TPT (1 μ M and 10 μ M) for 24 h. Cell pellets were lysed using radioimmune precipitation buffer containing protease inhibitors, and the concentration of protein was quantified using the Pierce BCA protein assay kit (Thermo Fisher Scientific, Inc., Waltham, MA, USA). A total of 10 micrograms of protein lysate was resolved on 4% to 20% gradient SDS-PAGE and transferred to a polyvinylidene difluoride membrane (Bio-Rad Inc., Hercules, CA) using a semidry transfer method. The membrane was probed with rabbit anti-SRSF6, rabbit anti-SRSF4 (Thermo Fisher Scientific, Inc., Waltham, MA, USA) and goat anti-cyclophilin A (Bio-Rad Inc., Hercules, CA) primary antibodies and horseradish peroxidase-conjugated goat anti-rabbit and donkey anti-goat (Bio-Rad Inc., Hercules, CA) secondary antibodies, respectively. Proteins were detected and quantified using the ChemiDoc MP Imaging System (Bio-Rad Inc., Hercules, CA). Band volumes for SRSF6 and SRSF4 were divided by band volumes for Cyclophilin A to normalize to housekeeping protein. For the purpose of graphical representation, percent expression in TPT-treated samples relative to DMSO was determined by dividing normalized band volumes in TPT-treated samples by DMSO-treated samples and multiplying by 100.

Statistical analyses. Viability data and percentages of different transcripts were analyzed using β regression modeling available in the *betareg* library (51) in the Bioconductor tool repository. DdPCR data normalized to *RPL27* and RNA yields were \log_2 transformed. Immunoblot data were normalized to cyclophilin A. Repeated measures analysis of variance (RM ANOVA) was implemented using library *nlme* (52) followed by *post hoc* Tukey test in all ddPCR, RNA yield and immunoblot comparisons that involved multiple TPT doses. Examination of residuals for each model was conducted using the *shapiro.test* function in R, indicating no large deviations from normality. Correlation analysis between *SRSF6* expression and proportion of GAG transcripts was conducted in GraphPad Prism software (GraphPad Software, La Jolla, CA, USA), using Spearman one-sided test, hypothesizing that higher expression of *SRSF6* is associated with accumulation of unspliced HIV transcripts. The effect of TPT on HIV reactivation using LRAs was assessed by comparing fold changes in expression between groups treated with TPT and LRAs versus LRAs alone. Fold changes were \log_2 transformed, and the normality of the distribution in each LRA- and LRA+TPT-treated group for MS and GAG was verified using *shapiro.test* function. The equal variance test was performed using function *var.test*. Based on the results of these tests, *t* test with equal or unequal variance was performed in cases where data distribution was normal, and Wilcoxon signed rank test otherwise. Because we hypothesized that TPT blocks HIV reactivation with LRAs, all these tests were one-sided. All graphs were constructed using GraphPad Prism software (GraphPad Software, La Jolla, CA, USA). Heatmaps were constructed using function *heatmap.2* from the library *gplots* in the R computing environment.

Data availability. RNA-Seq data for this work have been deposited in the Gene Expression Omnibus (GEO) under accession number [GSE215461](https://www.ncbi.nlm.nih.gov/geo/query/acc.cgi?acc=GSE215461).

SUPPLEMENTAL MATERIAL

Supplemental material is available online only.

SUPPLEMENTAL FILE 1, XLSX file, 1.7 MB.

SUPPLEMENTAL FILE 2, XLSX file, 0.04 MB.

SUPPLEMENTAL FILE 3, XLSX file, 0.02 MB.

ACKNOWLEDGMENTS

We thank Maile Karris and Deedee Pacheco and the San Diego CFAR [P30 AI036214] Clinical Investigation Core for recruiting study participants and providing peripheral blood samples. We thank the San Diego CFAR (P30 AI036214) Flow Cytometry Core for support in conducting cell sorting, and Genomics and Sequencing Core for assisting with and providing equipment for ddPCR experiments. We thank Cory White for discussions of the RNA-Seq data analyses. This research was supported by the grants from the National Institutes of Health HOPE Collaboratory UM1AI164559-01, AI100665, AI126620, and P30 AI036214, through the research infrastructure provided by the San Diego CFAR, and by the James B. Pendleton Charitable Trust. N.B.-B. was supported, in part, by a Career Developmental Award-II (IK2 BX002731) and the Merit Review Award (1I01 BX005285) from the Office of Research and Development, Veterans Health Administration, and AI157755 from the National Institutes of Health. This publication includes data generated at the UC San Diego IGM Genomics Center utilizing an Illumina NovaSeq 6000 that was purchased with funding from a National Institutes of Health SIG grant (#S10 OD026929). The views expressed in this article are those of the authors and do not necessarily reflect the position or policy of the Department of Veterans Affairs or the United States government. The sponsors of this research were not involved in the study design, collection or interpretation of the data, manuscript preparation, or the decision to submit the article for publication.

A.M., D.M.S., and N.B.-B. conceptualized the study and designed the experiments; A.M., S.D., and A.A.Q. performed the experiments; A.M., S.D., and N.B.-B. analyzed the data; A.M. and N.B.-B. wrote the manuscript; D.M.S. obtained funding to conduct the study. All authors participated in editing of the manuscript and approved the final version.

D.M.S. served as a consultant for Evidera, Matrix Biomed, Model Medicines, VxBio, Arena Pharmaceuticals, Pharma Holdings, and Bayer Pharmaceuticals; and served on the Scientific Advisory Board of Linear Therapies, Signant Health, and FluxErgy Inc. All other authors declare no conflict of interest.

REFERENCES

- Simonetti FR, Sobolewski MD, Fyne E, Shao W, Spindler J, Hattori J, Anderson EM, Watters SA, Hill S, Wu X, Wells D, Su L, Luke BT, Halvas EK, Besson G, Penrose KJ, Yang Z, Kwan RW, Van Waes C, Uldrick T, Citrin DE, Kovacs J, Polis MA, Rehm CA, Gorelick R, Piatak M, Keele BF, Kearney MF, Coffin JM, Hughes SH, Mellors JW, Maldarelli F. 2016. Clonally expanded CD4⁺ T cells can produce infectious HIV-1 in vivo. *Proc Natl Acad Sci U S A* 113:1883–1888. <https://doi.org/10.1073/pnas.1522675113>.
- Ishizaka A, Sato H, Nakamura H, Koga M, Kikuchi T, Hosoya N, Koibuchi T, Nomoto A, Kawana-Tachikawa A, Mizutani T. 2016. Short intracellular HIV-1 transcripts as biomarkers of residual immune activation in patients on antiretroviral therapy. *J Virol* 90:5665–5676. <https://doi.org/10.1128/JVI.03158-15>.
- Jordan A, Defechereux P, Verdin E. 2001. The site of HIV-1 integration in the human genome determines basal transcriptional activity and response to Tat transactivation. *EMBO J* 20:1726–1738. <https://doi.org/10.1093/emboj/20.7.1726>.
- Hunt PW, Brenchley J, Sinclair E, McCune JM, Roland M, Page-Shafer K, Hsue P, Emu B, Krone M, Lampiris H, Douek D, Martin JN, Deeks SG. 2008. Relationship between T cell activation and CD4⁺ T cell count in HIV-seropositive individuals with undetectable plasma HIV RNA levels in the absence of therapy. *J Infect Dis* 197:126–133. <https://doi.org/10.1086/524143>.
- Gallant J, Hsue PY, Shreay S, Meyer N. 2017. Comorbidities among US patients with prevalent HIV infection—a trend analysis. *J Infect Dis* 216:1525–1533. <https://doi.org/10.1093/infdis/jix518>.
- Kim Y, Anderson JL, Lewin SR. 2018. Getting the “kill” into “shock and kill”: strategies to eliminate latent HIV. *Cell Host Microbe* 23:14–26. <https://doi.org/10.1016/j.chom.2017.12.004>.
- Rasmussen TA, Lewin SR. 2016. Shocking HIV out of hiding: where are we with clinical trials of latency reversing agents? *Curr Opin HIV AIDS* 11:394–401. <https://doi.org/10.1097/COH.0000000000000279>.
- Vansant G, Bruggemans A, Janssens J, Debyser Z. 2020. Block-and-lock strategies to cure HIV infection. *Viruses* 12:84. <https://doi.org/10.3390/v12010084>.
- Gama L, Abreu CM, Shirk EN, Price SL, Li M, Laird GM, Pate KAM, Wietgrefe SW, O'Connor SL, Pianowski L, Haase AT, Van Lint C, Siliciano RF, Clements JE, L.-S. S. Group. 2017. Reactivation of simian immunodeficiency virus reservoirs in the brain of virally suppressed macaques. *AIDS* 31:5–14. <https://doi.org/10.1097/QAD.0000000000001267>.
- Garcia-Carbonero R, Supko JG. 2002. Current perspectives on the clinical experience, pharmacology, and continued development of the camptothecins. *Clin Cancer Res* 8:641–661.
- Li CJ, Zhang LJ, Dezube BJ, Crumpacker CS, Pardee AB. 1993. Three inhibitors of type 1 human immunodeficiency virus long terminal repeat-directed gene expression and virus replication. *Proc Natl Acad Sci U S A* 90:1839–1842. <https://doi.org/10.1073/pnas.90.5.1839>.
- Zhang JL, Sharma PL, Li CJ, Dezube BJ, Pardee AB, Crumpacker CS. 1997. Topotecan inhibits human immunodeficiency virus type 1 infection through a topoisomerase-independent mechanism in a cell line with altered topoisomerase I. *Antimicrob Agents Chemother* 41:977–981. <https://doi.org/10.1128/AAC.41.5.977>.
- Bennett RP, Stewart RA, Hogan PA, Ptak RG, Mankowski MK, Hartman TL, Buckheit RW, Jr, Snyder BA, Salter JD, Morales GA, Smith HC. 2016. An analog of camptothecin inactive against Topoisomerase I is broadly neutralizing of HIV-1 through inhibition of Vif-dependent APOBEC3G degradation. *Antiviral Res* 136:51–59. <https://doi.org/10.1016/j.antiviral.2016.11.001>.
- Beliakova-Bethell N, Mukim A, White CH, Deshmukh S, Abewe H, Richman DD, Spina CA. 2019. Histone deacetylase inhibitors induce complex host responses that contribute to differential potencies of these compounds in HIV reactivation. *J Biol Chem* 294:5576–5589. <https://doi.org/10.1074/jbc.RA118.005185>.
- Trypsteen W, White CH, Mukim A, Spina CA, De Spiegelaere W, Lefever S, Planelles V, Bosque A, Woelk CH, Vandekerckhove L, Beliakova-Bethell N. 2019. Long non-coding RNAs and latent HIV – A search for novel targets for latency reversal. *PLoS One* 14:e0224879. <https://doi.org/10.1371/journal.pone.0224879>.
- Spina CA, Anderson J, Archin NM, Bosque A, Chan J, Famiglietti M, Greene WC, Kashuba A, Lewin SR, Margolis DM, Mau M, Ruelas D, Saleh S, Shirakawa K, Siliciano RF, Singhania A, Soto PC, Terry VH, Verdin E, Woelk C, Wooden S, Xing S, Planelles V. 2013. An in-depth comparison of latent HIV-1 reactivation in multiple cell model systems and resting CD4⁺ T cells from aviremic patients. *PLoS Pathog* 9:e1003834. <https://doi.org/10.1371/journal.ppat.1003834>.
- Soto PC, Terry VH, Lewinski MK, Deshmukh S, Beliakova-Bethell N, Spina CA. 2022. HIV-1 latency is established preferentially in minimally activated and non-dividing cells during productive infection of primary CD4 T cells. *PLoS One* 17:e0271674. <https://doi.org/10.1371/journal.pone.0271674>.
- Sakabe NJ, de Souza SJ. 2007. Sequence features responsible for intron retention in human. *BMC genomics* 8:59–59. <https://doi.org/10.1186/1471-2164-8-59>.
- Popielarz M, Cavaloc Y, Mattei MG, Gattoni R, Stévenin J. 1995. The gene encoding human splicing factor 9G8: structure, chromosomal localization, and expression of alternatively processed transcripts. *J Biol Chem* 270:17830–17835. <https://doi.org/10.1074/jbc.270.30.17830>.
- Melhuish TA, Wotton D. 2006. The Tgif2 gene contains a retained intron within the coding sequence. *BMC Mol Biol* 7:2. <https://doi.org/10.1186/1471-2199-7-2>.
- Romano M, Marcucci R, Baralle FE. 2001. Splicing of constitutive upstream introns is essential for the recognition of intra-exonic suboptimal splice sites in the thrombopoietin gene. *Nucleic Acids Res* 29:886–894. <https://doi.org/10.1093/nar/29.4.886>.
- Michael IP, Kurlender L, Memari N, Yousef GM, Du D, Grass L, Stephan C, Jung K, Diamandis EP. 2005. Intron retention: a common splicing event within the human kallikrein gene family. *Clin Chem* 51:506–515. <https://doi.org/10.1373/clinchem.2004.042341>.
- Mahiet C, Swanson CM. 2016. Control of HIV-1 gene expression by SR proteins. *Biochem Soc Trans* 44:1417–1425. <https://doi.org/10.1042/BST20160113>.
- Tranell A, Fenyö EM, Schwartz S. 2010. Serine- and arginine-rich proteins 55 and 75 (SRp55 and SRp75) induce production of HIV-1 vpr mRNA by inhibiting the 5'-splice site of exon 3. *J Biol Chem* 285:31537–31547. <https://doi.org/10.1074/jbc.M109.077453>.
- Tranell A, Tingsborg S, Fenyö EM, Schwartz S. 2011. Inhibition of splicing by serine-arginine rich protein 55 (SRp55) causes the appearance of partially spliced HIV-1 mRNAs in the cytoplasm. *Virus Res* 157:82–91. <https://doi.org/10.1016/j.virusres.2011.02.010>.
- Elsheikh MM, Tang Y, Li D, Jiang G. 2019. Deep latency: a new insight into a functional HIV cure. *EBioMedicine* 45:624–629. <https://doi.org/10.1016/j.ebiom.2019.06.020>.
- Jean MJ, Hayashi T, Huang H, Brennan J, Simpson S, Purmal A, Gurova K, Keefer MC, Kobie JJ, Santoso NG, Zhu J. 2017. Curaxin CBL0100 blocks HIV-1 replication and reactivation through inhibition of viral transcriptional elongation. *Front Microbiol* 8:2007–2007. <https://doi.org/10.3389/fmicb.2017.02007>.
- Mousseau G, Kessing CF, Fromentin R, Trautmann L, Chomont N, Valente ST. 2015. The Tat inhibitor didehydro-cortistatin A prevents HIV-1 reactivation from latency. *mBio* 6:e00465. <https://doi.org/10.1128/mBio.00465-15>.

29. Li C, Mousseau G, Valente ST. 2019. Tat inhibition by didehydro-Cortistatin A promotes heterochromatin formation at the HIV-1 long terminal repeat. *Epigenetics Chromatin* 12:23–23. <https://doi.org/10.1186/s13072-019-0267-8>.
30. Zhou C-I, Huang Y-f, Li Y-b, Liang T-z, Zheng T-y, Chen P, Wu Z-y, Lai F-y, Liu S-w, Xi B-m, Li L. 2021. A new small-molecule compound, Q308, silences latent HIV-1 provirus by suppressing Tat- and FACT-mediated transcription. *Antimicrob Agents Chemother* 65:e00470-21. <https://doi.org/10.1128/AAC.00470-21>.
31. Mori L, Valente ST. 2020. Key players in HIV-1 transcriptional regulation: targets for a functional cure. *Viruses* 12:529. <https://doi.org/10.3390/v12050529>.
32. Lucera MB, Fleissner Z, Tabler CO, Schlatter DM, Troyer Z, Tilton JC. 2017. HIV signaling through CD4 and CCR5 activates Rho family GTPases that are required for optimal infection of primary CD4+ T cells. *Retrovirology* 14:4. <https://doi.org/10.1186/s12977-017-0328-7>.
33. Chen P, Flory E, Avots A, Jordan BW, Kirchhoff F, Ludwig S, Rapp UR. 2000. Transactivation of naturally occurring HIV-1 long terminal repeats by the JNK signaling pathway. The most frequent naturally occurring length polymorphism sequence introduces a novel binding site for AP-1 factors. *J Biol Chem* 275:20382–20390. <https://doi.org/10.1074/jbc.M001149200>.
34. Cameron PU, Saleh S, Sallmann G, Solomon A, Wightman F, Evans VA, Boucher G, Haddad EK, Sekaly R-P, Harman AN, Anderson JL, Jones KL, Mak J, Cunningham AL, Jaworowski A, Lewin SR. 2010. Establishment of HIV-1 latency in resting CD4+ T cells depends on chemokine-induced changes in the actin cytoskeleton. *Proc Natl Acad Sci U S A* 107:16934–16939. <https://doi.org/10.1073/pnas.1002894107>.
35. Williams SA, Greene WC. 2007. Regulation of HIV-1 latency by T-cell activation. *Cytokine* 39:63–74. <https://doi.org/10.1016/j.cyto.2007.05.017>.
36. Neueder A, Dumas AA, Benjamin AC, Bates GP. 2018. Regulatory mechanisms of incomplete huntingtin mRNA splicing. *Nat Commun* 9:3955. <https://doi.org/10.1038/s41467-018-06281-3>.
37. Royal W, Dupont B, McGuire D, Chang L, Goodkin K, Ernst T, Post MJ, Fish D, Pailloux G, Poncelet H, Concha M, Apuzzo L, Singer E. 2003. Topotecan in the treatment of acquired immunodeficiency syndrome-related progressive multifocal leukoencephalopathy. *J Neurovirol* 9:411–419. <https://doi.org/10.1080/713831540>.
38. Spina CA, Guatelli JC, Richman DD. 1995. Establishment of a stable, inducible form of human immunodeficiency virus type 1 DNA in quiescent CD4 lymphocytes in vitro. *J Virol* 69:2977–2988. <https://doi.org/10.1128/jvi.69.5.2977-2988.1995>.
39. Day JR, Martínez LE, Šašik R, Hitchin DL, Dueck ME, Richman DD, Guatelli JC. 2006. A computer-based, image-analysis method to quantify HIV-1 infection in a single-cycle infectious center assay. *J Virol Methods* 137:125–133. <https://doi.org/10.1016/j.jviromet.2006.06.019>.
40. Jordan A, Bisgrove D, Verdin E. 2003. HIV reproducibly establishes a latent infection after acute infection of T cells in vitro. *EMBO J* 22:1868–1877. <https://doi.org/10.1093/emboj/cdg188>.
41. Martin M. 2011. Cutadapt removes adapter sequences from high-throughput sequencing reads. *EMBnet j* 17:10–12. <https://doi.org/10.14806/ej.17.1.200>.
42. Kim D, Langmead B, Salzberg SL. 2015. HISAT: a fast spliced aligner with low memory requirements. *Nat Methods* 12:357–360. <https://doi.org/10.1038/nmeth.3317>.
43. Harrow J, Frankish A, Gonzalez JM, Tapanari E, Diekhans M, Kokocinski F, Aken BL, Barrell D, Zadissa A, Searle S, Barnes I, Bignell A, Boychenko V, Hunt T, Kay M, Mukherjee G, Rajan J, Despacio-Reyes G, Saunders G, Steward C, Harte R, Lin M, Howald C, Tanzer A, Derrien T, Chrast J, Walters N, Balasubramanian S, Pei B, Tress M, Rodriguez JM, Ezkurdia I, van Baren J, Brent M, Haussler D, Kellis M, Valencia A, Reymond A, Gerstein M, Guigó R, Hubbard TJ. 2012. GENCODE: the reference human genome annotation for The ENCODE Project. *Genome Res* 22:1760–1774. <https://doi.org/10.1101/gr.135350.111>.
44. Anders S, Pyl PT, Huber W. 2015. HTSeq—a Python framework to work with high-throughput sequencing data. *Bioinformatics* 31:166–169. <https://doi.org/10.1093/bioinformatics/btu638>.
45. Aanes H, Winata C, Moen LF, Østrup O, Mathavan S, Collas P, Rognes T, Aleström P. 2014. Normalization of RNA-sequencing data from samples with varying mRNA levels. *PLoS One* 9:e89158. <https://doi.org/10.1371/journal.pone.0089158>.
46. White CH, Moesker B, Beliakova-Bethell N, Martins LJ, Spina CA, Margolis DM, Richman DD, Planelles V, Bosque A, Woelk CH. 2016. Transcriptomic analysis implicates the p53 signaling pathway in the establishment of HIV-1 latency in central memory CD4 T cells in an In vitro model. *PLoS Pathog* 12:e1006026. <https://doi.org/10.1371/journal.ppat.1006026>.
47. Robinson MD, McCarthy DJ, Smyth GK. 2010. EdgeR: a bioconductor package for differential expression analysis of digital gene expression data. *Bioinformatics* 26:139–140. <https://doi.org/10.1093/bioinformatics/btp616>.
48. Benjamini Y, Hochberg Y. 1995. Controlling the false discovery rate: a practical and powerful approach to multiple testing. *J R Stat Soc, B MET* 57:289–300. <https://doi.org/10.1111/j.2517-6161.1995.tb02031.x>.
49. Sherman BT, Hao M, Qiu J, Jiao X, Baseler MW, Lane HC, Imamichi T, Chang W. 2022. DAVID: a web server for functional enrichment analysis and functional annotation of gene lists (2021 update). *Nucleic Acids Res* 50:W216–W221. <https://doi.org/10.1093/nar/gkac194>.
50. Lawrence M, Huber W, Pagès H, Aboyoun P, Carlson M, Gentleman R, Morgan MT, Carey VJ. 2013. Software for computing and annotating genomic ranges. *PLoS Comput Biol* 9:e1003118. <https://doi.org/10.1371/journal.pcbi.1003118>.
51. Cribari-Neto F, Zeileis A. 2010. Beta regression in R. *J Stat Softw* 34:1–24.
52. Pinheiro J, Bates D, DebRoy S, Sarkar D, Team RC. 2016. nlme: linear and nonlinear mixed effects models. R package version 3.1–127.